Interactions of the Sponge-Derived Antimitotic Tripeptide Hemiasterlin with Tubulin: Comparison with Dolastatin 10 and Cryptophycin 1

Ruoli Bai,[‡] Neil A. Durso,[§] Dan L. Sackett,[§] and Ernest Hamel*[,§]

Science Applications International Corporation−Frederick, National Cancer Institute, Frederick Cancer Research and Development Center, Frederick, Maryland 21702, Laboratory of Drug Discovery Research and Development, Developmental Therapeutics Program, Division of Cancer Treatment and Diagnosis, National Cancer Institute, Frederick Cancer Research and Development Center, Frederick, Maryland 21702

Received June 9, 1999; Revised Manuscript Received August 19, 1999

ABSTRACT: The sponge-derived antimitotic tripeptide hemiasterlin was previously shown to inhibit tubulin polymerization. We have now demonstrated that hemiasterlin resembles most other antimitotic peptides in noncompetitively inhibiting the binding of vinblastine to tubulin (apparent K_i value, 7.0 μM), competitively inhibiting the binding of dolastatin 10 to tubulin (apparent K_i value, 2.0 μM), stabilizing the colchicine binding activity of tubulin, inhibiting nucleotide exchange on β-tubulin, and inducing the formation of tubulin oligomers that are stable to gel filtration in the absence of free drug, even at low drug concentrations. The tubulin oligomerization reaction induced by hemiasterlin was compared to the reactions induced by dolastatin 10 and cryptophycin 1. Like dolastatin 10, hemiasterlin induced formation of a tubulin aggregate that had the morphological appearance primarily of ring-like structures with a diameter of about 40 nm, while the morphology of the cryptophycin 1 aggregate consisted primarily of smaller rings (diameter about 30 nm). However, the hemiasterlin aggregate differed from the dolastatin 10 aggregate in that its formation was not associated with turbidity development, and the morphology of the hemiasterlin aggregate (as opposed to the dolastatin 10 aggregate) did not change greatly when microtubule-associated proteins were present (tight coils and pinwheels are observed with dolastatin 10 but not with hemiasterlin or cryptophycin 1). Opacification of tubulin−dolastatin 10 mixtures was inhibited by hemiasterlin at 22 °C and stimulated at 0 °C, while cryptophycin 1 was inhibitory at both reaction temperatures.

Naturally occurring small peptides, many of marine origin and all possessing modified amino acids, are among the most potent compounds that inhibit microtubule assembly. Although there is an imperfect correlation between the biochemical and cytological properties of these agents, most members of this class of drug display high binding affinities for tubulin and markedly potent inhibitory effects on cell growth (for a review, see ref *1*). Many of these peptides are active against human xenograft tumors in immunodeficient mice, and, consequently, at least three (dolastatin 10, cryptophycin 52, and Cemadotin[1]) are in clinical trials for the treatment of human cancer (*2*−*4*).

Hemiasterlin (structure in Figure 1, together with those of dolastatin 10, chiral "isomer 2" of dolastatin 10, and cryptophycin 1) and closely related analogues are the newest additions to this peptide family. Hemiasterlin and closely related compounds have been repeatedly isolated from marine sponges (*5*−*7*), and Anderson et al. (*8*) found that hemiasterlin arrested cells in mitosis and caused the disappearance of intracellular microtubules. Ireland (*9*) reported that the tripeptide inhibited tubulin assembly and was a noncompetitive inhibitor of the binding of radiolabeled vinblastine to tubulin.

Most recently, cytotoxic fractions from the Papua New Guinea sponges *Auletta* sp. and *Siphonochalina* spp. yielded hemiasterlin and smaller amounts of related peptides (*10*). The potent cytotoxicity of hemiasterlin was confirmed, with the lowest IC_{50} values (about 2 pM) being obtained in the human tumor cell lines OVCAR-3 and NCI-H460, and we, too, found that hemiasterlin strongly inhibited tubulin assembly, with activity intermediate between that of dolastatin 10 and cryptophycin 1 (IC_{50} values of 0.59, 0.98, and 1.1 μM for dolastatin 10, hemiasterlin, and cryptophycin 1, respectively). In the present study, we have analyzed the tubulin−hemiasterlin interaction in greater detail. In particular, we have focused on how hemiasterlin affects the binding of other ligands to tubulin and on differences between the tubulin aggregation reactions promoted by hemiasterlin, dolastatin 10, and cryptophycin 1.

MATERIALS AND METHODS

Materials. Electrophoretically homogeneous bovine brain tubulin, heat-treated MAPs[2] (*11*), tubulin freed of unbound nucleotide, used in experiments in which the binding of [8-^{14}C]GTP to tubulin was examined (*12*), and [^{3}H]dolastatin 10 (*13*) were prepared as described previously. Hemiasterlin

* Address correspondence to this author at NCI−FCRDC, P.O. Box B, Bldg 469, Room 237, Frederick, MD 21702-1201. Telephone: (301) 846-1678. FAX: (301) 846-6775. Email: hamele@dc37a.nci.nih.gov.

[‡] Science Applications International Corporation−Frederick.

[§] Laboratory of Drug Discovery Research and Development, Developmental Therapeutics Program.

[1] Cryptophycin 52 and Cemadotin are synthetic analogues of the naturally occurring cryptophycin 1 and dolastatin 15, respectively.

10.1021/bi991323e CCC: $18.00
Published on Web 10/08/1999

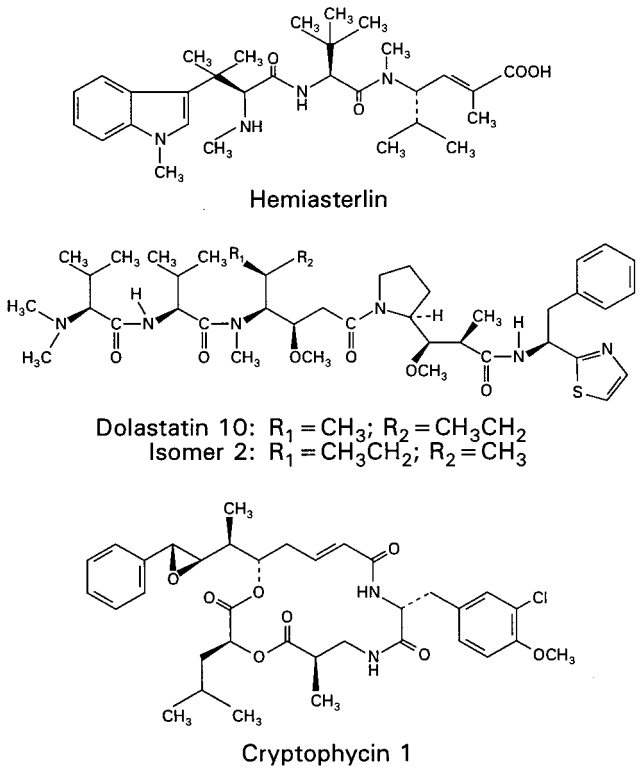

FIGURE 1: Structural formulas of hemiasterlin, dolastatin 10, chiral isomer 2 of dolastatin 10, and cryptophycin 1.

(*10*) was generously provided by our NCI colleague Dr. W. R. Gamble. Synthetic dolastatin 10 (*14*) and its chiral isomer 2 (*15*) were generously provided by Dr. G. R. Pettit and cryptophycin 1 (*16*) by Merck Research Laboratories. GTP (Sigma) and [8-^{14}C]GTP (Moravek Biochemicals) were repurified by anion exchange chromatography on DEAE-cellulose by elution with triethylammonium bicarbonate gradients. Maytansine and rhizoxin were provided by the Drug Synthesis and Chemistry Branch, National Cancer Institute, and [^{3}H]vinblastine and [^{3}H]colchicine were from Amersham and NEN-Dupont, respectively.

Methods. The binding of [^{3}H]dolastatin 10, [^{3}H]vinblastine, or [8-^{14}C]GTP to tubulin was measured by centrifugal gel filtration on 1.0 mL columns of Sephadex G-50 (superfine) prepared in tuberculin syringe barrels as described previously (*17, 18*). Columns were equilibrated with and experiments were performed in a solution containing 0.1 M Mes (pH 6.9 with NaOH in 1 M stock solution) and 0.5 mM $MgCl_2$. The binding of [^{3}H]colchicine to tubulin was measured using the DEAE-cellulose filter technique and the reaction conditions of Ludueña et al. (*19*).

For electron microscopy, 0.25 mL reaction mixtures were incubated for about 30 min at 37 °C and followed turbidimetrically. About 10 μL was taken from each mixture and applied to carbon-coated, Formavar-treated 200-mesh copper grids. The sample droplet was immediately washed from the grid by 5−10 drops of 0.5% (w/v) uranyl acetate, and excess stain was wicked from the grid with torn filter paper. The grids were examined in a Zeiss model 10CA electron microscope. Reaction mixtures contained tubulin at 10 μM (1.0 mg/mL), drug at 20 μM, 4% (v/v) dimethyl sulfoxide, 0.1 M Mes (pH 6.9), 0.5 mM $MgCl_2$, and, if present, heat-treated MAPs at 0.5 mg/mL.

HPLC was performed on two Shodex Protein KW-803 columns (8 × 300 mm) in series protected by a TosoHaas TSK-GEL SW guard column (7.5 × 75 mm). The columns were equilibrated and developed with a solution containing 0.1 M Mes (pH 6.9) and 0.5 mM $MgCl_2$, and samples were prepared in the same solution. All samples (0.25 mL) contained tubulin at 2.5 μM (0.25 mg/mL) and 1% dimethyl sulfoxide. Flow rate was 0.7 mL/min. Void volume (19.9 min) was determined with blue dextran (2000 kDa).

Turbidimetry was measured in Gilford model 250 recording spectrophotometers equipped with electronic temperature controllers. The 0.25 mL reaction mixtures contained 0.1 M Mes (pH 6.9), 0.5 mM $MgCl_2$, 4% dimethyl sulfoxide, and tubulin and drugs as indicated. Reaction mixtures were equilibrated at the experimental temperature before addition of drug(s), the last component(s) added. If two drugs were added, dolastatin 10 was added immediately after the hemiasterlin or cryptophycin 1.

Table 1: Inhibition by Hemiasterlin and Other Vinca Domain Drugs of the Binding of [^{3}H]Vinblastine and [^{3}H]Dolastatin 10 to Tubulin[a]

drug added	% inhibition of [^{3}H]vinblastine binding	% inhibition of [^{3}H]dolastatin 10 binding
hemiasterlin	27	43
dolastatin 10	44	
cryptophycin 1	36	42
vinblastine		2
maytansine	33	25
rhizoxin	12	3

[a] The 0.4 mL reaction mixtures contained 10 μM tubulin, 0.5% dimethyl sulfoxide, the indicated potential inhibitor at 5.0 μM, and either [^{3}H]vinblastine or [^{3}H]dolastatin 10 at 10 μM. Incubation was for 30 min, and centrifugal gel filtrations of duplicate 0.19 mL aliquots were at room temperature. Averages from two independent experiments are presented in the table. Stoichiometry of binding in the control reaction mixtures: 0.57 mol of vinblastine and 0.59 mol of dolastatin 10 per mole of tubulin.

RESULTS

Inhibition of Vinblastine Binding to Tubulin by Hemiasterlin. We first wanted to confirm the report (*9*) that hemiasterlin, like the previously studied peptide antimitotic drugs dolastatin 10 (apparent K_i versus vincristine, 1.4 μM; ref *17*), phomopsin A (apparent K_i versus vincristine, 2.8 μM; ref *17*), and cryptophycin 1 (apparent K_i versus vinblastine, 3.9 μM; ref *18*), was a noncompetitive inhibitor of the binding of radiolabeled vinca alkaloids to tubulin. An initial experiment demonstrated that hemiasterlin was active as an inhibitor of vinblastine binding (Table 1), and more extensive experiments confirmed that the inhibition was noncompetitive (Figure 2). The data of Figure 2 are presented in the Hanes format,[3] with noncompetitive inhibition indicated when curves generated at different substrate and inhibitor concentrations intercept on the negative *x*-axis (*20*).

[2] Abbreviations: MAPs, microtubule-associated proteins; Mes, 4-morpholineethanesulfonate; HPLC, high-performance liquid chromatography.

[3] Note that for the studies presented here and below with [^{3}H]-dolastatin 10, a stoichiometric drug binding assay is being analyzed by methods originally devised for analysis of catalytic enzyme reactions, where both substrate and inhibitor are present in large molar excess to the enzyme.

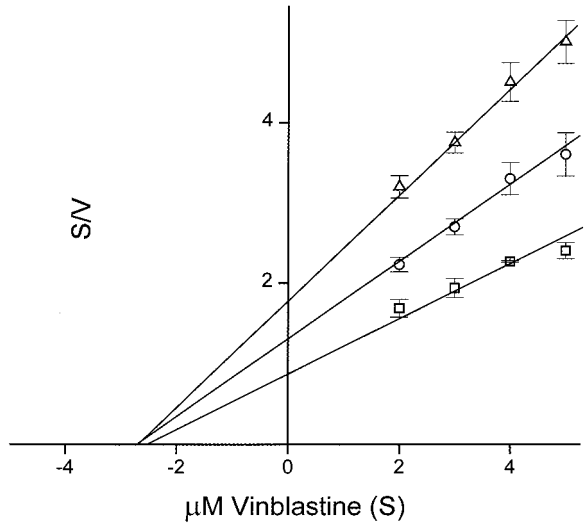

FIGURE 2: Hanes analysis of the inhibition of binding of [^{3}H]-vinblastine to tubulin by hemiasterlin. Reaction mixtures (0.4 mL) contained 1.0 mg/mL (10 μM) tubulin, 0.1 M Mes, 0.5 mM $MgCl_2$, 1% dimethyl sulfoxide, [^{3}H]vinblastine as indicated, and hemiasterlin as follows: □, none; ○, 4.0 μM; △, 8.0 μM. Incubation was for 30 min at room temperature (22−23 °C). Data of two experiments were averaged, with duplicate 0.15 mL aliquots of each reaction mixture in each experiment applied to room-temperature syringe-columns of Sephadex G-50 (superfine). Centrifugal gel filtration was at room temperature. Standard deviations are shown. Lines drawn by linear regression, using Origin Microcal Version 4.1. Ordinate units: (μM vinblastine) (μg of tubulin) (pmol of vinblastine bound)$^{-1}$.

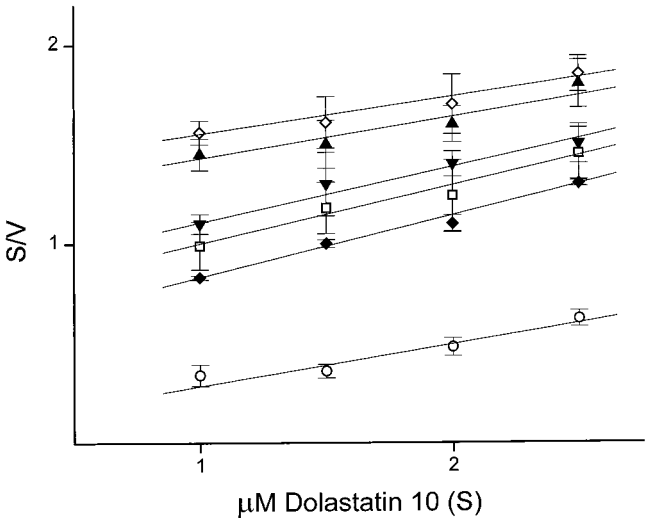

FIGURE 3: Hanes analysis of the inhibition of binding of [^{3}H]-dolastatin 10 to tubulin by hemiasterlin and dolastatin 10 chiral isomer 2. Reaction mixtures (0.4 mL) contained 0.25 mg/mL (2.5 μM) tubulin, 0.1 M Mes, 0.5 mM $MgCl_2$, 1% dimethyl sulfoxide, [^{3}H]dolastatin 10 as indicated, and inhibitor as follows: ○, none; ◆, 4.0 μM hemiasterlin; ▼, 6.0 μM hemiasterlin; ▲, 8.0 μM hemiasterlin; □, 2.0 μM isomer 2; ◇, 4.0 μM isomer 2. Incubation was for 2 h at room temperature (22−23 °C). Data of two experiments were averaged, with duplicate 0.15 mL aliquots of each reaction mixture in each experiment applied to room-temperature syringe-columns of Sephadex G-50 (superfine). Centrifugal gel filtration was at room temperature. Standard deviations are shown. Lines drawn by linear regression, using Origin Microcal Version 4.1. Ordinate units: (μM dolastatin 10) (μg of tubulin) (pmol of dolastatin 10 bound)$^{-1}$.

Dixon analysis (*20*) of these and similar data yielded an apparent K_i for hemiasterlin of 7.0 μM.

Inhibition of Dolastatin 10 Binding to Tubulin by Hemiasterlin. In previous studies, we had obtained data indicating that the dolastatin 10 chiral isomer 2 (structure in Figure 1; apparent K_i, 0.8 μM; ref *21*) and cryptophycin 1 (apparent K_i, 2.1 μM; ref *18*) competitively inhibit the binding of radiolabeled dolastatin 10 to tubulin. An initial experiment (Table 1) showed that hemiasterlin strongly inhibited the binding of [^{3}H]dolastatin 10 to tubulin. This was followed by detailed studies, including a contemporaneous reevaluation of isomer 2, and we found that both hemiasterlin and isomer 2 competitively inhibited the binding of [^{3}H]dolastatin 10 to tubulin (Figure 3). The data obtained with both compounds yielded the parallel curves generated by competitive inhibitors by Hanes analysis (*20*). These and similar data yielded apparent K_i values of 2.0 μM for hemiasterlin and 0.7 μM for isomer 2 versus [^{3}H]dolastatin 10.

Stabilization of the Colchicine Binding Activity of Tubulin by Hemiasterlin. The temperature- and time-dependent decay of the colchicine binding activity of tubulin has been described by many workers (e.g., refs *19*, *22*−*25*). Many drugs that interfere with the binding of vinca alkaloids to tubulin stabilize the ability of the protein to bind colchicine, even appearing to enhance colchicine binding, and stabilization appears to correlate with the ability of drugs to induce formation of oligomers and polymers of tubulin with aberrant (i.e., nonmicrotubule) morphology. The peptide antimitotics are particularly potent in their ability to stabilize colchicine binding (*17*−*19*). As shown in Table 2, hemiasterlin, like dolastatin 10 and cryptophycin 1, prevented any loss of the ability of tubulin to bind colchicine following a 3 h preincubation at 37 °C. The enhanced binding of colchicine without a preincubation, previously observed with dolastatin 10 and cryptophycin 1, also occurred with hemiasterlin.

Table 2: Stabilization of the Colchicine Binding Activity of Tubulin by Hemiasterlin, Dolastatin 10, and Cryptophycin 1[a]

	colchicine bound (% rel to unpreincubated control ± SD)	
drug added	no preincubation	preincubation
none	100	68 ± 14
hemiasterlin	165 ± 4	162 ± 22
dolastatin 10	165 ± 4	153 ± 22
cryptophycin 1	146 ± 4	142 ± 25

[a] The reaction conditions of Ludueña et al. (*19*) were used to measure the binding of 50 μM [^{3}H]colchicine to 40 μM tubulin. Preincubated samples were incubated 3 h at 37 °C prior to addition of colchicine. Incubation with colchicine was for 2 h at 37 °C. The control value was 0.34 pmol of [^{3}H]colchicine bound/pmol of tubulin.

Inhibition of Nucleotide Exchange on Tubulin by Hemiasterlin. All drugs that interfere with vinca alkaloid binding to tubulin, whether or not they cause aberrant assembly reactions, inhibit nucleotide exchange on tubulin. Because the nucleotide exchange reaction is so rapid (*26*), this inhibition requires that drug be added to tubulin prior to addition of radiolabeled nucleotide (*27*). The peptide antimitotics are particularly effective inhibitors of the nucleotide exchange reaction, although in the case of cryptophycin 1 maximum inhibition of nucleotide exchange required a lengthy drug−tubulin preincubation prior to addition of GTP (*18*).

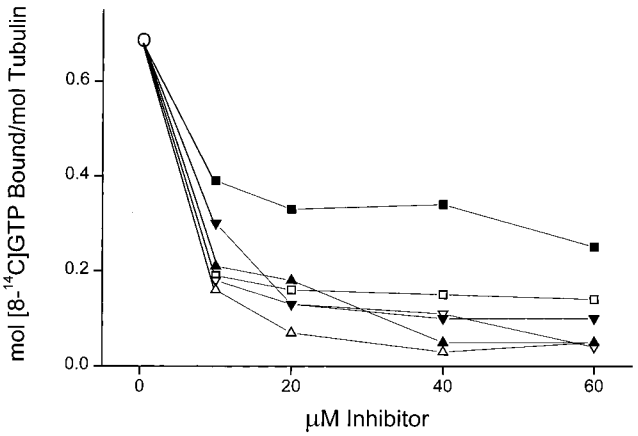

FIGURE 4: Comparison of the inhibitory effects of hemiasterlin, dolastatin 10, and cryptophycin 1 on the binding of [8-^{14}C]GTP to tubulin. Each 0.4 mL reaction mixture contained 1.0 mg/mL (10 μM) tubulin, 0.1 M Mes, 0.5 mM $MgCl_2$, 2% dimethyl sulfoxide, 50 μM [8-^{14}C]GTP, and the indicated concentrations of hemiasterlin (inverted triangles), dolastatin 10 (upright triangles), or cryptophycin 1 (squares). The value obtained without drug (no preincubation) is indicated by the open circle. [8-^{14}C]GTP was always the last ingredient added to the reaction mixtures. The solid symbols indicate the nucleotide was added immediately after the drug, while the open symbols indicate that drug preceded nucleotide by 1 h. Following GTP addition, reaction mixtures were left on ice for 30 min, at which time duplicate 0.15 mL aliquots of each reaction mixture were applied to cold syringe-columns of Sephadex G-50 (superfine). Centrifugal gel filtration was at 4 °C.

Figure 4 shows that hemiasterlin more closely resembles dolastatin 10 than cryptophycin 1 in its effects on the nucleotide exchange. Although the parameter measured in this experiment is the binding of [8-^{14}C]GTP to tubulin, the reaction includes displacement of exchangeable-site nonradiolabeled GDP purified with the tubulin. Except with 10 μM hemiasterlin, binding of [8-^{14}C]GTP was nearly as extensive when the radiolabled nucleotide was added to the tubulin immediately after either dolastatin 10 or hemiasterlin as when drug was added an hour later. In experiments with tubulin initially bearing [8-^{14}C]GDP in the exchangeable site, addition of hemiasterlin prior to addition of nonradiolabeled GTP prevented displacement of radiolabeled nucleotide from the protein (data not presented). Thus, as with other drugs binding in the vinca domain (including dolastatin 10 and cryptophycin 1), hemiasterlin interferes with the nucleotide exchange reaction rather than actually binding in the exchangeable site.

Hemiasterlin Induces Formation of Apparently Stable Tubulin Oligomers. Although HPLC gel permeation chromatography was initially developed as a Hummel−Dryer method to study the interaction of vinca alkaloids with tubulin (*28*), with the columns equilibrated with free drug, we have found the method valuable for studying the oligomerization reaction of tubulin $\alpha\beta$-dimers in the presence of antimitotic peptides (*17, 18*). These agents are generally available only in scant amounts, and thus it is impractical to equilibrate the columns prior to application of the tubulin sample. Tubulin oligomers formed even with low concentrations of these drugs seem stable during the gel filtration procedure, consistent with very slow drug dissociation reactions.

To enhance resolution of the tubulin species formed in the presence of different drug concentrations, we used two

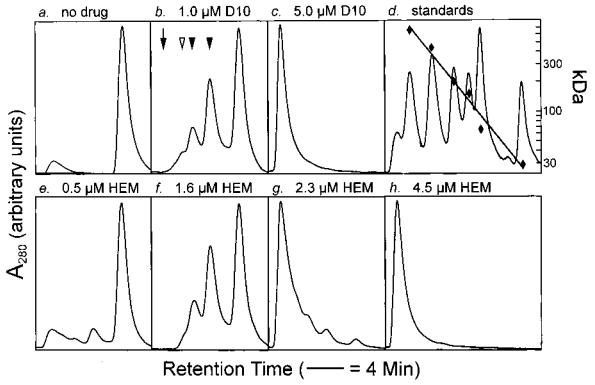

FIGURE 5: Size exclusion HPLC of tubulin incubated with dolastatin 10 (D10) or hemiasterlin (HEM). Reaction mixtures containing the indicated concentrations of drug were incubated 20 min at room temperature prior to injection into the HPLC system. The retention times for the void volume (arrow, panel b) and $\alpha\beta$-tubulin dimer were 19.9 and 27.9 min, respectively. Panel d presents a tracing combining six protein standards (from Sigma) in amounts (0.06−0.20 mg/mL) to yield peaks of similar A_{280}. These proteins were bovine erythrocyte carbonic anhydrase (29 kDa), bovine serum albumin (66 kDa), yeast alcohol dehydrogenase (150 kDa), sweet potato β-amylase (200 kDa), horse spleen apoferritin (443 kDa), and bovine thyroglobulin (669 kDa).

columns in series (Figure 5). This did not appear to increase the number of distinct peaks (cf. refs *17, 18*), but they were better resolved. Figure 5a presents a typical elution pattern observed in the absence of drug. The small peak near the void volume probably represents denatured tubulin, as it increased following incubation of reaction mixtures without drug, and occasionally it was not observed. Figure 5b and Figure 5c demonstrate the effects of low (1.0 μM) and high (5.0 μM) concentrations of dolastatin 10, respectively, relative to the tubulin concentration of 2.5 μM. Figures 5e−h show the effects of hemiasterlin concentrations ranging from 0.5 to 4.5 μM. We did not observe a significant quantitative difference between the effects of dolastatin 10 and hemiasterlin in this series of experiments [previously we had found similar quantitative effects when dolastatin 10 and phomopsin A were compared (*17*) and when dolastatin 10 and cryptophycin 1 were compared (*18*)]. As in the earlier studies, increasing drug concentration led to a progressive increase in oligomer size, with two species appearing as distinct peaks within the included volume (closed arrowheads in Figure 5b) and a third that has generally had the appearance of a shoulder (open arrowhead, Figure 5b). When the drug concentration was equivalent to or higher than the tubulin concentration, most or all of the protein was recovered in the void volume (arrow, Figure 5b).

Figure 5d shows the elution pattern of a mixture of six protein standards, with a semilogarithmic plot of their molecular masses superimposed on the elution profile. By this calibration, the tubulin $\alpha\beta$-dimer eluted at a time corresponding to 115 kDa, and the three oligomeric species at times corresponding to 270, 460, and 590 kDa. This suggests that these species may correspond to 2 (2.3), 4, and 5 (5.1) $\alpha\beta$-dimers, respectively. The absence of an apparent $\alpha\beta$-tubulin trimer may indicate that this species is unstable or that addition of $\alpha\beta$-dimer doublets in the growth of larger oligomers can occur.

Morphological Evaluation of Tubulin Aggregates Formed in the Presence of Hemiasterlin. In previous electron

microscopic studies, we found that higher concentrations of dolastatin 10 (*13*) and cryptophycin 1 (*18*) led to formation of extensive tubulin aggregation products of defined and aberrant morphology. The aggregates formed by the two drugs differed markedly in their appearances (larger rings and broken rings with dolastatin 10, clusters of smaller rings with cryptophycin 1). Additionally, the morphology of the dolastatin 10-induced aggregate, but not of the cryptophycin 1-induced aggregate, changed substantially in the presence of MAPs (with dolastatin 10, tight coils and pinwheel-like aggregates were observed among clusters of the larger rings). The aggregate we observed with cryptophycin 1 differed little in appearance from that described by other workers. Kerksiek et al. (*29*) observed aggregate following addition of cryptophycin 1 to preformed microtubules, with the protofilaments appearing to disassemble directly into the aggregate, and Smith and Zhang (*30*) described aggregate formation following addition of cryptophycin 1 to unpolymerized microtubule protein.

The aggregation of tubulin induced by hemiasterlin described above led us to perform electron microscopic studies with this drug (Figure 6), with a simultaneous comparison with the effects of dolastatin 10 and cryptophycin 1. Aggregates formed without MAPs are shown in panel A, and those with MAPs in panel B. The appearances of the dolastatin 10- and cryptophycin 1-induced aggregates were essentially identical to those reported previously,[4] and the reader will find micrographs for comparison in refs *13* and *18*.

In all cases except for the dolastatin 10/+ MAPs condition, there appeared to be large aggregate clusters with an underlying repetitive ring structure of fairly uniform morphology best visualized at the clump edges, together with abundant conjoined and single rings in the spaces between the larger clusters. Broken rings, double rings, and more linear filaments were also observed.

As previously described (*13*), when MAPs were included with dolastatin 10, tight coils and pinwheels appeared among the rings. The rings observed with cryptophycin 1 were distinctly smaller than those formed with either dolastatin 10 or hemiasterlin. Restricting the measurements, made on electron micrographs at 300 000-fold magnification, to discrete, well-resolved rings (that is, ignoring double rings, ring aggregates, and incomplete rings), average ring outer diameters without MAPs were 42 ± 2 (SD) nm with hemiasterlin and with dolastatin 10 and 27 ± 1 nm with cryptophycin 1. With MAPs, ring diameters were virtually the same: 42 ± 2 nm with hemiasterlin, 41 ± 2 nm with dolastatin 10, and 26 ± 2 nm with cryptophycin 1. Preliminary studies by analytical ultracentrifugation and measurement of ring diffusion coefficients are consistent with these measurements.

The hemiasterlin aggregates seem morphologically more closely related to the dolastatin 10 aggregates than to the cryptophycin 1 aggregates (see refs *13* and *18)*, except for the following observations. First, the overall appearance of the hemiasterlin aggregate is almost unaffected by addition of MAPs, except that in the presence of MAPs double rings were more frequently observed. Second, in several independently prepared specimens with hemiasterlin, we have never observed the tight coils and pinwheels that form in the dolastatin 10/+ MAPs system. Third, with hemiasterlin, as with cryptophycin 1, turbidity development was not observed visually following addition of drug to tubulin solutions, as compared with the intense turbidity that develops when dolastatin 10 and tubulin are mixed (see next section).

Limited Aberrant Polymerization with Hemiasterlin and Effects of the Tripeptide on the Dolastatin 10-Induced Aberrant Polymerization. As noted previously (*18*), when tubulin and dolastatin 10 are mixed, a time-dependent aberrant polymerization reaction occurs.[5] This is characterized by opacification of the reaction mixture, and the reaction can be followed turbidimetrically in the same manner as a standard tubulin assembly reaction. Investigations (unpublished) of this reaction have demonstrated that it has a temperature optimum at 22 °C, among the temperatures studied (0, 10, 22, 30, and 37 °C), and that most of the polymer formed ultimately settles to the bottom of the cuvette. This effect of dolastatin 10 was first noted in ligand binding assays, but no turbidity change was observed with either cryptophycin 1 or hemiasterlin.

Figure 7 shows the failure of hemiasterlin or cryptophycin 1 to cause turbidity development and the time course of the dolastatin 10-induced reaction at two tubulin and drug concentrations (10 or 20 μM of both components). After a relatively long period at a plateau, the turbidity reading in each sample with dolastatin 10 began to decline slowly, with this apparent loss in turbidity more marked in the 20 μM tubulin−drug sample. Visual examination of the cuvettes revealed that this was due to settling of the polymer, as opposed to its disassembly. The Figure 7 inset is a photograph of identical 20 μM samples after about 30 min at room temperature (lanes 1−4), as well as of a dolastatin 10 sample after 2 h at room temperature (lane 5).

We previously had shown that cryptophycin 1 inhibited turbidity development induced by dolastatin 10 (*18*). Figure 8A confirms this finding and demonstrates that at 22 °C hemiasterlin has a similar effect, although hemiasterlin was significantly less potent than cryptophycin 1.

We have begun a more extensive investigation of the aberrant polymerization and oligomerization reactions induced by these antimitotic peptides. We have found an apparent optimum for the dolastatin 10-induced reaction at 22 °C. At lower reaction pH and higher Mg^{2+} concentrations, turbidity development occurs with hemiasterlin or cryptophycin 1, but these reactions are maximal at 0 °C and decline progressively as reaction temperature is increased. When we examined hemiasterlin and cryptophycin 1 for inhibitory effects on dolastatin 10-induced polymerization at 0 °C (Figure 8B), very different results were obtained as compared with the experiment at 22 °C (Figure 8A). In particular,

[4] The only significant difference was with dolastatin 10 without MAPs. In previous studies, the aggregate morphology had the appearance of a sheet of rings and broken rings over the entire grid. In the current studies, there were discrete clumps of aggregate, as seen with both hemiasterlin and cryptophycin 1 as well, with rings particularly well visualized at the edges of the clumps and in interstices between clumps.

[5] For purposes of this discussion, "polymerization" will specifically indicate drug-induced formation of aggregate of discrete morphology that causes turbidity development, while "oligomerization" will indicate formation of apparently smaller multimeric species detected by other means (e.g., HPLC, analytical ultracentrifugation, multiangle light scattering).

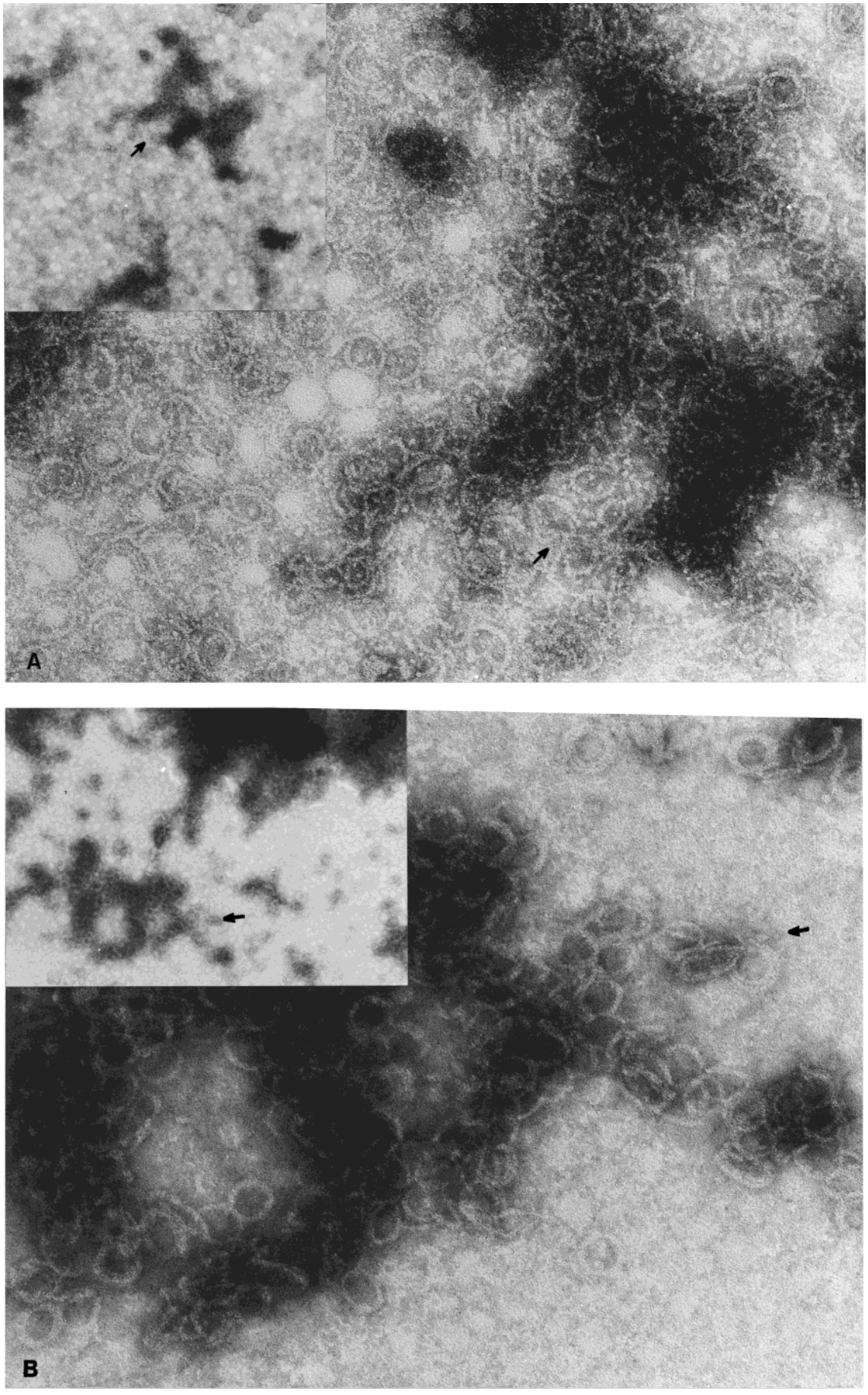

FIGURE 6: Morphology of tubulin aggregates induced by hemiasterlin in the absence (A) and presence (B) of MAPs. Magnifications: × 180000× (main panels) and × 36000× (insets). The arrows indicate similar positions in the low and high power views.

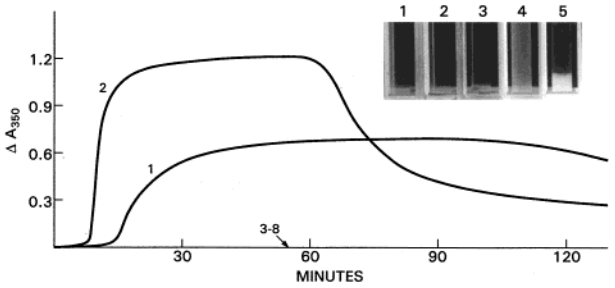

FIGURE 7: Aberrant tubulin polymerization, as manifested by turbidity development, induced by dolastatin 10. The reaction mixture represented by curve 1 contained both tubulin and dolastatin 10 at 10 μM, and that represented by curve 2 contained both components at 20 μM. Reaction temperature was 22 °C, and dolastatin 10 was added to each sample at zero time. No change in turbidity occurred in the absence of drug or in the presence of either hemiasterlin or cryptophycin 1 at both tubulin and drug concentrations (curves 3−8). The inset shows 0.5 mL samples (lower halves of cuvettes) incubated at room temperature for 30 min (cuvettes 1−4) or 2 h (cuvette 5) containing 20 μM tubulin and either no drug (cuvette 1), 20 μM hemiasterlin (cuvette 2), 20 μM cryptophycin 1 (cuvette 3), or 20 μM dolastatin 10 (cuvettes 4 and 5).

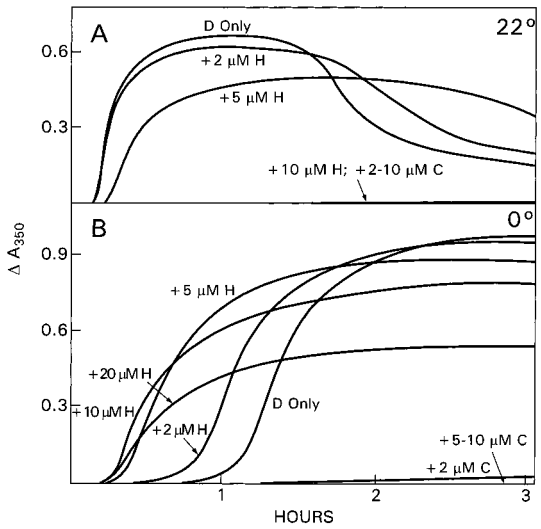

FIGURE 8: Effects of hemiasterlin and cryptophycin 1 on the aberrant tubulin polymerization induced by dolastatin 10. (A) The 22 °C reaction. Each reaction mixture contained 10 μM tubulin and 10 μM dolastatin 10. The curve labeled "D Only" represents the reaction that occurred without any further addition. Other reaction mixtures also contained 2−10 μM hemiasterlin (H) or 2−10 μM cryptophycin 1 (C), as indicated. The base line position for each sample was first established prior to drug addition, with a small adjustment made following drug addition after verification that no significant change in turbidity had occurred. (B) The 0 °C reaction. Each reaction mixture contained 10 μM tubulin and 10 μM dolastatin 10. The curve labeled "D Only" represents the reaction that occurred without any further addition. Other reaction mixtures also contained 2−20 μM hemiasterlin (H) or 2−10 μM cryptophycin 1 (C), as indicated. The base line position for each sample was established as described for panel A.

hemiasterlin stimulated the dolastatin 10 reaction (itself more sluggish at 0 °C than at 22 °C), with an apparent maximal effect at about 10 μM (that is, with tubulin, hemiasterlin, and dolastatin 10 all equimolar). Furthermore, concentrations of hemiasterlin alone that exceeded the tubulin concentration caused very slow turbidity development (not shown). The effects of cryptophycin 1, in contrast, were unchanged. The depsipeptide alone caused no change in turbidity (not shown), and it continued to potently inhibit the dolastatin 10-induced polymerization reaction.

DISCUSSION

Isolated first by Talpir et al. (*5*), then by Coleman et al. (*7*), and most recently by Gamble et al. (*10*) from a variety of tropical sponge species, hemiasterlin is thus far, structurally, the simplest of the highly cytotoxic antimitotic peptides and depsipeptides. This study was initiated to determine similarities and differences between the effects of hemiasterlin, dolastatin 10, and cryptophycin 1 on tubulin.

The three peptides, as well as phomopsin A, probably bind in a site distinct from that at which the vinca alkaloids bind, since they all noncompetitively inhibit the binding of radiolabeled vinca alkaloids to tubulin. In contrast, hemiasterlin as well as cryptophycin 1 and chiral isomer 2 of dolastatin 10 (*18*, *21*) competitively inhibit the binding of [^{3}H]dolastatin 10 to tubulin. This implies a common binding site, which we have called the "peptide site" (*17*).

Hemiasterlin, like dolastatin 10, cryptophycin 1, and phomopsin A, potently stabilizes the colchicine binding activity of tubulin. This effect, we believe, can be attributed to the structurally aberrant, highly stable tubulin oligopolymers that form in the presence of these peptides (based on observation of oligomer persistence during size exclusion chromatography and apparently quantitative retention of very low concentrations of [^{3}H]dolastatin 10 in oligomer peaks; see refs *13*, *17*, *18*). Vinblastine, which induces formation of less stable tubulin oligomers (based on their apparent disintegration during size exclusion HPLC in the absence of free drug; unpublished), stabilizes colchicine binding less potently than the peptides. Finally, all drugs that inhibit vinblastine binding without inducing oligomer formation (maytansine, rhizoxin, halichondrin B, spongistatin 1) have no ability to stabilize the colchicine site (*17*−*19*, *31*, *32*).

The three peptides also inhibit nucleotide exchange on tubulin, but do not bind in the exchangeable GTP site. The effect of hemiasterlin more closely resembles that of dolastatin 10 than that of cryptophycin 1, in that it does not appear to be greatly affected by a drug−tubulin preincubation [although observing this effect requires that drug be added to tubulin prior to addition of radiolabeled nucleotide, presumably because of the rapidity of the nucleotide exchange reaction (*26*)]. While inhibition of nucleotide exchange could derive from peptide-induced oligopolymer formation, similar inhibition of nucleotide exchange occurs with the inhibitors of vinblastine binding that do not induce oligomer formation (*17*, *27*). Moreover, inhibition of nucleotide exchange is minimal in the presence of vinblastine, even at drug concentrations that should lead to extensive spiral formation (*17*, *27*).

The three peptides share a common ability to induce formation of oligomers of tubulin that are apparently stable during size exclusion HPLC, while vinblastine-induced oligomers dissociate in the absence of free drug during HPLC. The HPLC studies with substoichiometric drug concentrations indicate that the initial stages of the oligomerization are similar with the three drugs, both qualitatively and quantitatively, but resolution of peaks is not adequate for detection of subtle conformational differences or, perhaps, to resolve all early intermediates.

By electron microscopy the three peptides appear to induce formation of large aggregates with a primarily ring-like substructure. In previous studies, primarily with dolastatin 10, we have not observed qualitative morphological changes with varying drug and tubulin concentrations, as a function of reaction temperature, or with addition of GTP to reaction mixtures (*13*).

Nevertheless, it is in these aggregation reactions that the three peptides show the greatest differences in their interactions with tubulin. From the studies performed thus far, there are three major, but interrelated, differences meriting mention: first, morphological features of the oligopolymers; second, the effects of MAPs on morphology; and, third, the differing turbidimetric effects of the drugs.

At first glance, the hemiasterlin oligomers appear to be morphologically very similar to those induced by dolastatin 10, in that the average ring diameter is the same. However, there was minimal change in morphology with hemiasterlin when MAPs were added to the reaction mixture, and hemiasterlin caused no turbidity development in reaction mixtures after prolonged incubation at 22 °C. Similarly, cryptophycin 1 oligomer morphology was unaltered with MAPs and the depsipeptide did not cause turbidity development; but the morphology of the cryptophycin 1-induced oligomer was quite distinct from those formed with hemiasterlin or dolastatin 10.

Cryptophycin 1 and hemiasterlin also displayed quite distinct effects on the dolastatin 10-induced polymerization reaction. At 22 °C, both compounds inhibited the dolastatin 10 reaction, cryptophycin 1 more potently than hemiasterlin. When the reaction temperature was reduced to 0 °C, cryptophycin 1 remained strongly inhibitory, but hemiasterlin appeared to enhance the reaction. The results suggest assembly of a mixed polymer containing both peptides that forms preferentially at the colder temperature.

The failure of both hemiasterlin and cryptophycin 1 to cause turbidity development with tubulin puzzles us in view of the large aggregates present on the electron microscope grids. It is possible that this apparent clumping represents an artifact that arises in placing the sample on the grid or from its interaction with the uranyl acetate stain, with the individual rings representing the true structures formed with hemiasterlin and cryptophycin 1.[6] Preliminary centrifugal pelleting studies are consistent with this view, in that pellets were only formed with the dolastatin 10-induced polymer (relative to controls without drug, both with and without MAPs) following low-speed centrifugation[7] (not unexpected, in view of the polymer's settling properties at 1*g*). Pellet formation with hemiasterlin, relative to the control without drug, but not with cryptophycin 1, did occur following high-speed centrifugation,[8] but this phenomenon could simply result from the difference in size of unaggregated rings formed with the two drugs.

Only with dolastatin 10 + MAPs have we observed repeatedly in the electron microscope polymers which have an unambiguous coiled structure. We are reluctant to attribute the turbidity development observed with dolastatin 10 to these coils, however, since they are not observed without MAPs, and turbidity development without MAPs is substantially greater than that with MAPs in reaction mixtures containing the same concentrations of tubulin and dolastatin 10. Moreover, we have noted with interest the recent observation of the polymerization of bacterial FtsZ protein into polymers 7−20 nm in width (versus the 25 nm diameter of microtubules) without turbidity development (*33*). We are presently evaluating peptide effects by other modalities to gain a greater understanding of subtle differences in the way these compounds interact with tubulin and in the aberrant morphology of the structures formed in their presence.

[6] In the study of Kerksiek et al. (*29*) with cryptophycin 1, however, the drug was added to preformed microtubules, and an oligopolymer of clumped rings, morphologically indistinguishable from the clumped rings described here, seemed to unravel from microtubule ends.

[7] Eppendorf 5417C centrifuge, 5000 and 14 000 rpm for 20 min.

[8] Beckman TLA 100.1 rotor in TL-100 centrifuge, 85 000 rpm for 30 min.

REFERENCES

1. Hamel, E. (1996) *Med. Res. Rev. 16*, 207−231.
2. Bagniewski, P. G., Reid, J. M., Pitot, H. C., Sloan, J. A., and Ames, M. M. (1997) *Proc. Am. Assoc. Cancer Res. 38*, 221−222.
3. Allen, S. L., Villalona-Calero, M., Jakimowicz, K., Fram, R., O'Mara, V., Kolitz, J. E., Gallagher, M. A., Van Echo, D., Fischkoff, S., and O'Dwyer, P. (1997) *Proc. Am. Assoc. Cancer Res. 38*, 222.
4. Stevenson, J. P., Gallagher, M., Vaughn, D., Schucter, L., Haller, D., Fox, K., Algazy, K., Aviles, V., Hahn, S., and O'Dwyer, P. J. (1999) *Proc. Am. Assoc. Cancer Res. 40*, 92.
5. Talpir, R., Benayahu, Y., Kashman, Y., Pannell, L., and Schleyer, M. (1994) *Tetrahedron Lett. 35*, 4453−4456.
6. Crews, P., Farias, J. J., Emrich, R., and Keifer, P. A. (1994) *J. Org. Chem. 59*, 2932−2934.
7. Coleman, J. E., de Silva, E. D., Kong, F., Andersen, R. J., and Allen, T. M. (1995) *Tetrahedron 39*, 10653−10662.
8. Anderson, H. J., Coleman, J. E., Andersen, R. J., and Roberge, M. (1997) *Cancer Chemother. Pharmacol. 39*, 223−226.
9. Ireland, C. M. (1997) Presentation at the Fourth Anticancer Drug Discovery and Development Symposium, Annapolis, MD.
10. Gamble, W. R., Durso, N. A., Fuller, R. W., Westergaard, C. K., Johnson, T. R., Sackett, D. L., Hamel, E., Cardellina, J. H., II, and Boyd, M. R. (1999) *Bioorg. Med. Chem. 7*, 1611−1615.
11. Hamel, E., and Lin, C. M. (1984) *Biochemistry 23*, 4173−4184.
12. Grover, S., and Hamel, E. (1994) *Eur. J. Biochem. 222*, 163−172.
13. Bai, R., Taylor, G. F., Schmidt, J. M., Williams, M. D., Kepler, J. A., Pettit, G. R., and Hamel, E. (1995) *Mol. Pharmacol. 47*, 965−976.
14. Pettit, G. R., Singh, S. B., Hogan, F., Lloyd-Williams, P., Herald, D. L., Burkett, D. D., and Clewlow, P. J. (1989) *J. Am. Chem. Soc. 111*, 5463−5465.
15. Pettit, G. R., Singh, S. B., Hogan, F., and Burkett, D. D. (1990) *J. Med. Chem. 33*, 3132−3133.
16. Schwartz, R. E., Hirsch, C. F., Sesin, D. F., Flor, J. E., Chartrain, M., Fromtling, R. E., Harris, G. H., Salvatore, M. J., Liesch, J. M., and Yudin, K. (1990) *J. Ind. Microbiol. 5*, 113−124.
17. Bai, R., Pettit, G. R., and Hamel, E. (1990) *J. Biol. Chem. 265*, 17141−17149.
18. Bai, R., Schwartz, R. E., Kepler, J. A., Pettit, G. R., and Hamel, E. (1996) *Cancer Res. 56*, 4398−4406.
19. Ludueña, R. F., Prasad, V., Roach, M. C., and Lacey, E. (1989) *Arch. Biochem. Biophys. 272*, 32−38.
20. Dixon, M., Webb, E. C., Thorne, C. J. R., and Tipton, K. F. (1979) *Enzymes*, 3rd ed., Academic Press, New York.
21. Bai, R., Taylor, G. F., Cichacz, Z. A., Herald, C. L., Kepler, J. A., Pettit, G. R., and Hamel, E. (1995) *Biochemistry 34*, 9714−9719.
22. Weisenberg, R. C., Borisy, G. G., and Taylor, E. W. (1968) *Biochemistry 7*, 4466−4477.

23. Wilson, L. (1970) *Biochemistry 9*, 4999−5007.
24. Frigon, R. P., and Lee, J. C. (1972) *Arch. Biochem. Biophys. 153*, 587−589.
25. Barton, J. S. (1978) *Biochim. Biophys. Acta 532*, 155−160.
26. Brylawski, B. P., and Caplow, M. (1983) *J. Biol. Chem. 258*, 760−763.
27. Huang, A. B., Lin, C. M., and Hamel, E. (1985) *Biochem. Biophys. Res. Commun. 128*, 1239−1246.
28. Singer, W. D., Hersh, R. T., and Himes, R. H. (1988) *Biochem. Pharmacol. 37*, 2691−2696.
29. Kerksiek, K., Mejillano, M. R., Schwartz, R. E., Georg, G. I., and Himes, R. H. (1995) *FEBS Lett. 377*, 59−61.
30. Smith, C. D., and Zhang, X. (1996) *J. Biol. Chem. 271*, 6192−6198.
31. Mandelbaum-Shavit, F., Wolpert-DeFilippes, M. K., and Johns, D. G. (1976) *Biochem. Biophys. Res. Commun. 72*, 47−54.
32. Bhattacharyya, B., and Wolff, J. (1977) *FEBS Lett. 75*, 159−162.
33. Mukherjee, A., and Lutkenhaus, J. (1999) *J. Bacteriol. 181*, 823−832.

BI991323E